

Track to track fusion method applied to road obstacle detection

C. Blanc **L. Trassoudaine**
LASMEA, UMR 6602 du CNRS
Campus des Cézeaux
63173 Aubière Cedex
France

cblanc, trassou@lasmea.univ-bpclermont.fr

Y. Le Guilloux **R. Moreira**
SAGEM SA
Division Défense et Sécurité
95100 Argenteuil
France

yann.leguilloux, raphael.moreira@sagem.com

Abstract – This paper presents a data fusion Kalman based method applied to obstacle detection in road situations. We describe the principle and the implementation of fusion process. It is based on tracks produced separately by single sensors. Results with Infrared and Radar sensors are shown, proving the benefit of this dual approach. Another application with Radar and LIDAR is also illustrated.

Keywords: Intelligent vehicles, data fusion, tracking, situation analysis, obstacle detection, Infrared, Radar, LIDAR.

1 Introduction

Perception is critical for Intelligent Vehicles for they must generally cope with an unknown environment. As widely illustrated over the past years [1, 2, 3], using more than one sensor can greatly improve perception performance, provided that the problem of data fusion is solved. This is a major issue in multiple sensors co-operation. It can be divided into sub-problems:

- Space of measurements: different sensors measure different properties of the environment; we first have to find a common space of measurements to compare data,
- Data synchronisation: basically, sensors are asynchronous; therefore a synchronisation step is necessary before any kind of fusion process,
- Fusion strategy: choice depends on the sensors, the available data, and the goal of the system; the fusion is clearly correlated with the representation of measurements.

Finally, a multisensor system takes advantage of the complementarity of sensors and is more robust to adverse conditions (weather, unavailability of one sensor), more accurate and reliable.

In this paper, we propose a data fusion scheme for obstacle detection in section 2. Section 3 describes two concrete applications of data fusion. The first application, from the PAROTO project, is devoted to obstacle avoidance using a Radar and an Infrared camera. The second application deals with Radar / LIDAR data fusion for obstacle detection.

2 Track fusion system

The data fusion scheme proposed here is fitted to the problem of obstacle detection ahead of a vehicle. This problem can be seen as follows: each sensor produces tracks, mapped onto the 2D representation (see figure 1). Fusion is done on these 2D tracks (obstacles are loosely classified).

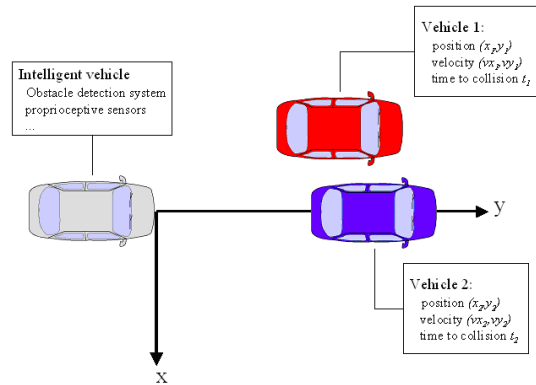


Fig. 1: An obstacle detection problem representation

2.1 Fusion system architecture

This section describes the fusion module and its functions. Figure 2 illustrates the sequence of operations performed by the fusion module (top-down). The following requires a few definitions: *sensor tracks* - as provided by sensors - can either be matched to tracks from the alternate sensor, thus forming 'couples' referred to as *dual-mode tracks*, or stay unmatched - *monomode tracks* ('singles'). First, the module starts receiving new information from any sensor (i.e. sensor track updates).

2.2 Data flow management

2.2.1 monomode

Then it updates its own sensor track database (carry on, create, delete) to reflect input information. Obviously, newly created tracks are monomode tracks.

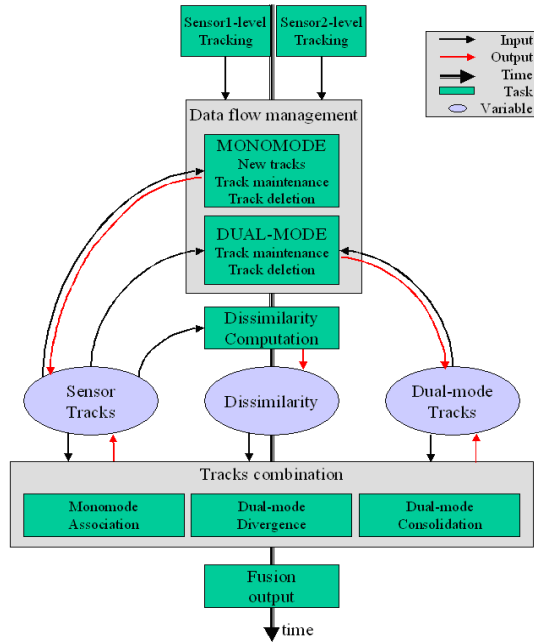


Fig. 2: schema fusion module

2.2.2 dual-mode

Now the dual-mode ('couple') database is updated, so that whenever any member of a dual-mode track was deleted in the previous step, the dual-mode track no longer holds, and the matching sensor track turns back to monomode ('widow').

2.3 Track dissimilarity computation

Tracks association from different sensors is a crucial step in the track fusion process. Several association methods have been presented in [4]. We use a gating procedure which is enough for correct assignments. Sensor tracks are maintained by Kalman filters, and extrapolated to the most recent date. Then if any pair of tracks from alternate sensors fall within the common observation area (referred to below as *dual-mode area*), the projection of their states onto a common measurement space $\tilde{x}^1(k)$ and $\tilde{x}^2(k)$, together with corresponding covariance matrices $p^1(k)$ and $p^2(k)$, are used to compute a dissimilarity level.

We shall note $\Delta^{12} = \tilde{x}^1(k) - \tilde{x}^2(k)$. We need to design a test to select between two hypotheses [4]:

$$H_0 : \Delta^{12} = 0$$

and

$$H_1 : \Delta^{12} \neq 0$$

Assuming that errors are gaussian and independent, covariance of Δ^{12} is:

$$p^{12}(k) = p^1(k) + p^2(k)$$

H_0 is true if $\Delta^{12}(k)' [p^{12}(k)]^{-1} \Delta^{12}(k) \leq \delta$ where δ is a parameter given from tables of chi-square distribution. The value

$$misfit = \Delta^{12}(k)' [p^{12}(k)]^{-1} \Delta^{12}(k)$$

is called track dissimilarity.

2.4 Track combination

2.4.1 monomode association

When the dissimilarity between two monomode tracks from different sensors is below some threshold, they are candidates for a match. The best candidate pairs are then matched into dual-mode tracks.

2.4.2 dual-mode consolidation

The purpose of our tracking association is to improve our knowledge of dual-mode tracks using independent data sources. Thus, we carry out a Kalman filter at the fusion level, whose observations are the sensor-level tracking inputs, i.e. Z_k^1 and Z_k^2 .

Let us consider the target state vector:

$$X^{12} = \begin{pmatrix} x_{12} \\ \dot{x}_{12} \\ y_{12} \\ \dot{y}_{12} \end{pmatrix}$$

where x_{12}, y_{12} are the target position in the common sensors reference, and $\dot{x}_{12}, \dot{y}_{12}$ the target relative speed. Kinematics model can be represented in matrix form as:

$$X_{k+1}^{12} = F X_k^{12} + G V_k, V_k \sim N(0, Q_k)$$

where F is the transition matrix which models the evolution of X_k^{12} , and Q_k the covariance matrix of V_k which is modeled by acceleration.

$$F = \begin{pmatrix} 1 & T & 0 & 0 \\ 0 & 1 & 0 & 0 \\ 0 & 0 & 1 & T \\ 0 & 0 & 0 & 1 \end{pmatrix} G = \begin{pmatrix} T^2/2 & 0 \\ T & 0 \\ 0 & T^2/2 \\ 0 & T \end{pmatrix}$$

$$Q_k = \begin{pmatrix} \sigma_{ax_{12}}^2 & 0 \\ 0 & \sigma_{ay_{12}}^2 \end{pmatrix}$$

The fusion method considered is illustrated by figure 3 and was inspired from work of J.B. Gao and C.J. Harris [5].

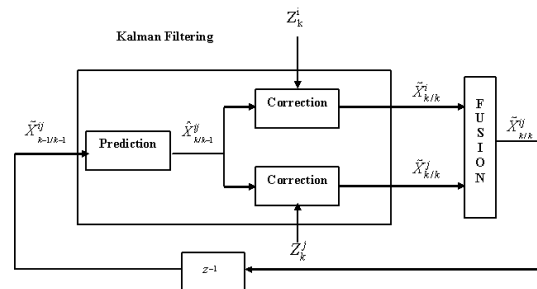


Fig. 3: kalman fusion module

$\tilde{X}_{k-1/k-1}^{12}$ is the fused state estimate. Its prediction is:

$$\hat{X}_{k/k-1}^{12} = F\tilde{X}_{k-1/k-1}^{12}$$

The prediction is associated to measurements Z_k^1 and Z_k^2 in order to obtain two estimated states $\tilde{X}_{k/k}^1$ and $\tilde{X}_{k/k}^2$ by using local Kalman filters.

Measurements equations are derived from the following model:

$$\hat{Z}_{k/k-1}^i = H^i \hat{X}_{k/k-1}^{12} + W_k^i, W_k^i \sim N(0, R_k^i)$$

where $\hat{Z}_{k/k-1}^i$ is the predicted measurement vector, H^i the measurement sensitivity matrix, and R_k^i the covariance matrix of W_k^i for sensor i .

For each sensor there is classically the estimated state vector:

$$\tilde{X}_{k/k}^i = \hat{X}_{k/k-1}^i + K_k^i [Z_k^i - \hat{Z}_{k/k-1}^i]$$

where K_k^i is gain Kalman gain for sensor i .

Finally, the new fused state estimate is given by:

$$\tilde{X}_{k/k}^{12} = \tilde{X}_{k/k}^1 + [\tilde{P}_{k/k}^1 - \tilde{P}_{k/k}^{12}][\tilde{P}_{k/k}^1 + \tilde{P}_{k/k}^2 - \tilde{P}_{k/k}^{12} - \tilde{P}_{k/k}^{21}]^{-1}(\tilde{X}_{k/k}^1 - \tilde{X}_{k/k}^2)$$

where $\tilde{P}_{k/k}^1$ and $\tilde{P}_{k/k}^2$ are the associated covariance matrix of estimates $\tilde{X}_{k/k}^1$ and $\tilde{X}_{k/k}^2$.

$\tilde{P}_{k/k}^{12} = (\tilde{P}_{k/k}^{21})^t$ is the cross-covariance matrix of $\tilde{X}_{k/k}^1$ and $\tilde{X}_{k/k}^2$. The covariance matrix of the fused estimate is given by:

$$\tilde{P}_{k/k}^{\prime 12} = \tilde{P}_{k/k}^1 - [\tilde{P}_{k/k}^1 - \tilde{P}_{k/k}^{12}][\tilde{P}_{k/k}^1 + \tilde{P}_{k/k}^2 - \tilde{P}_{k/k}^{12} - \tilde{P}_{k/k}^{21}]^{-1}[\tilde{P}_{k/k}^1 - \tilde{P}_{k/k}^2]$$

2.4.3 dual-mode divergence

It is important to detect whenever sensor tracks belonging to a dual-mode track drift away from each other with time. This is achieved by checking their distance from the consolidated state of the dual-mode track they belong to. We have:

$$p_k^{12} = \tilde{P}_{k/k}^1 + \tilde{P}_{k/k}^2 - \tilde{P}_{k/k}^{12} - \tilde{P}_{k/k}^{21}$$

For each sensor the validation gate is given by [6]:

$$\left\{ Z_k^i, (\hat{Z}_{k/k-1}^i - Z_k^i)^t S^{i-1} (\hat{Z}_{k/k-1}^i - Z_k^i) \leq \gamma_i \right\}$$

where

$$S^{i-1} = H^i \tilde{P}_{k/k-1}^{\prime 12} H^{i t} + R_k^i$$

and

$$\tilde{P}_{k/k-1}^{\prime 12} = F \tilde{P}_{k-1/k-1}^{\prime 12} F^t + G Q_k G^t$$

2.5 Fusion output

The fusion module output includes:

- All the dual-mode tracks; they correspond to obstacles detected by both sensors in the dual-mode area,

- Monomode tracks belonging to area only covered by the originating sensor. This area is noted as exclusive area.

Since the perception fields in the 2D map depend on the sensors properties and their location on the vehicle, they will be illustrated for each application described in the following.

At this point, if a monomode track remains in the dual-mode area, we interpret it as either a false detection of one sensor or a miss of the other sensor.

The decision to output such a track from the fusion module depends on the confidence level associated with each single sensor. Therefore, this part of the fusion module should be customised depending on the application.

3 Applications

3.1 Fusing Radar and IR tracking

The Radar / IR data fusion has been implemented within the PAROTO project ([7, 8, 9]). The goal of the project is to develop a system, fitted on a standard car, able to prevent collisions by anticipating the presence of hazardous obstacles ahead. Radar and IR camera are complementary sen-



Fig. 4: VELAC equipped with IR and Radar

sors: Radar being able to give accurate distance and speed of an obstacle, and the IR camera delivering a good bearing estimate.

3.1.1 Radar specifications and tracking results

The key interests to use a Radar in this project are on the one hand the accuracy of obstacles estimated speed and distance, and on the other hand the quality of radar data up to 150 m in spite of bad weather conditions. According to the regulation in the European Union and in the United States, the wave emission frequency for an anti-collision project is fixed to $f_0 = 77GHz$ (millimetre wave).

The principle of the Radar used in this framework is a pulsed Doppler Radar with a Doppler priority. Indeed, the priority is given to the speed of obstacles with respect to the experimental vehicle. The distance of the obstacles are sorted by P range gates.

Moreover, this Radar has only one antenna for both emission and reception which provide a 3.3° field of view. This system requires a circulator (ultra-high-frequency system) and a synchronisation process in order to transfer the energy either between the transmitter and the antenna

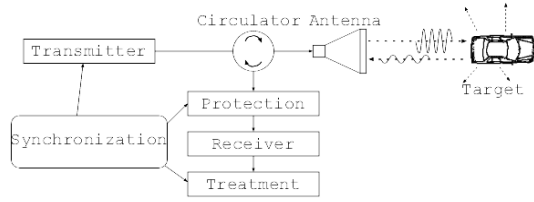


Fig. 5: Structure of the PAROTO Radar with one antenna

or between the antenna and the receiver (figure 5). The reception channel being very sensitive, the system must perfectly isolate this channel from the emission one because of the strong emitted power.

The Radar technique used in this project consists in sending by repetitive pulses (width $t_e = 150ns$ and period $T_r = 4\mu s$) a sinusoidal electromagnetic wave and to receive and analyse the signal reflected by a target (figure 6). The data resolution is:

- for range:

$$\delta D = ct_e/2 = 3 \times 10^8 \times 150 \times 10^{-9}/2 = 22.5m$$

- for speed:

$$\delta v = \frac{c}{2 \times f_0 \times T_r \times N} = \frac{3 \times 10^8}{2 \times 77 \times 10^9 \times 4 \times 10^{-6} \times 2048} = 0.238m/s$$

where N represents the period number (at the moment 2048 which correspond to $8ms$ of time analysis) of the pulse repetition T_r .

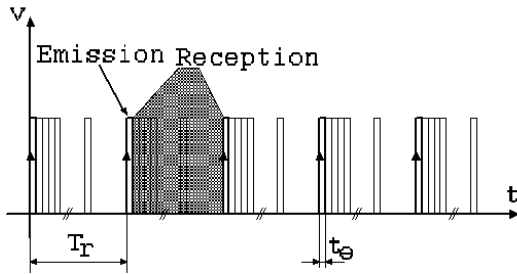


Fig. 6: Emission and reception chart

First, echo extraction is done: the process acquires, each $n \times T_r$ ($n \in [0, \dots, N - 1]$) time, an array of data corresponding to the sample of the two I, Q reflected signals ($0^\circ, 90^\circ$) provided by a high speed $40MHz$ two line converter stage. Then an estimation of the power spectral density is computed by FFT (Fast Fourier Transform) analysis. In this new array, we apply a threshold clustering algorithm and extract echoes. An echo is then defined by four parameters:

- time: $n \times T_r, n \in [0, \dots, N - 1]$
- amplitude: value of the power spectral density versus frequency

- Doppler: position in the column power spectral density array

$$V_r = (column - \frac{N}{2}) * \delta v$$

- range: position in the line power spectral density array

$$r = (line - 1) \times \delta D + \frac{\delta D}{2}$$

A constant velocity model is used into a Kalman filter to track echoes. This tracking is performed in three steps:

- initialisation of tracks (r, V_r) using coherence in many frames ,
- filtering of tracks: prediction and estimation,
- data association.

This tracking yields a more accurate range estimate than the gate value ($22.5m$). Obstacle speed is also filtered. Results are shown figure 7 in foggy condition (obstacle is invisible for a human driver)

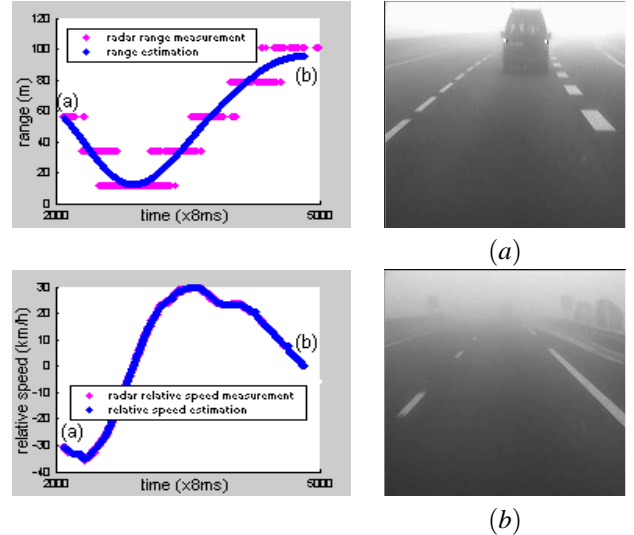


Fig. 7: obstacle in foggy condition (visible domain images)

3.1.2 IR camera specification and tracking results

Our infrared sensor is an uncooled 8-12 micro bolometer. Its thermal resolution is 80 mK. The size of images is 320×240 pixels. The optical design allows a $40^\circ \times 30^\circ$ field of view. The camera is located on top of the windscreen, for practical and theoretical reasons (dirt, projections and geometry of distance estimation).

In classical road situations, the sources of danger relate to human activity. This leads us to focus the detection on vehicles, cycles and pedestrians, which exhibit strong and typical behaviours in infrared.

The IR processing results are obstacle image positions. In order to recover 3D positions from 2D image positions, we assume that the road belongs to a plane, and perform back-projection and derive (x, y) (note : $z = 0$). Therefore, (x, y) observations are fed into a constant velocity Kalman filter,

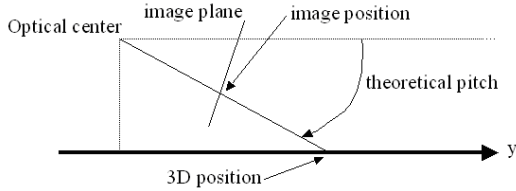


Fig. 8: Side view

which maintains $X^1 = (x_1, \dot{x}_1, y_1, \dot{y}_1)^t$ state vectors. Since backprojection is sensitive to the changes of pitch, motion analysis - based on feature tracking - is performed in order to refine the pitch estimate and correct 3D positions accordingly. Some results are shown in figure 9.



Fig. 9: Some IR processing results

3.1.3 Data fusion and results

We have to customise the fusion module for the application.

Fusion area Detection characteristics of our sensors are summarised in table 1:

	range	field of view
Radar	150m	3.3°
Infrared	75m	60°

Table 1: Detection characteristics of our sensors

Therefore, figure 10 illustrates it, Radar detects obstacles up to a distance of 150 m along the axis of the vehicle, whereas Infrared sees vehicles even coming sideways.

Moreover, the dual-mode area yields top detection performance in the space that the vehicle is about to occupy shortly, which is of utmost importance.

Monomode tracks in dual-mode area Our experience of the PAROTO system taught us that Radar processing gives no miss and sometimes detects irrelevant objects, like bridges. Infrared processing gives only few false detections in the dual-mode area, and only very short detection gaps. These observations lead us to consider monomode tracks in dual-mode area as false detections, hence discarded from outputs.

Areas of fusion to consider Radar and infrared cover complementary areas ahead of the vehicle (figure 10). We call a track or an area dual-mode when both sensors are involved. Tracks produced by single processes lie in one of the three areas described in figure 10. If an IR (resp. Radar) track is produced in the IR (resp. Radar) exclusive area, the fusion module cannot confirm it with a track from the other sensor process: it must rely on this single sensor. In the other hand, if the track is produced in the dual mode

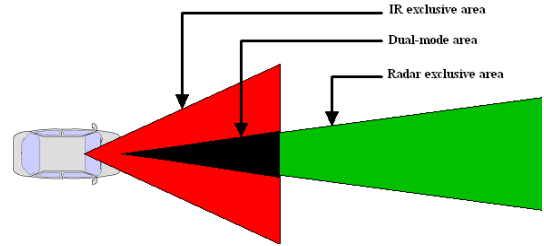


Fig. 10: Areas covered by PAROTO system

area, a real data fusion can be performed.

Outputs of the data fusion We illustrate here some situations and show that fusion gives a significant gain in respect with separate sensor processing.

Simple situation On figure 11, we observe two vehicles in the image. After sensor processing, IR and Radar send to the fusion module the produced tracks. As expected, IR tracks are less accurate in distance than Radar tracks, and errors on IR measures grow with distance, whereas direction estimates are more accurate in IR.

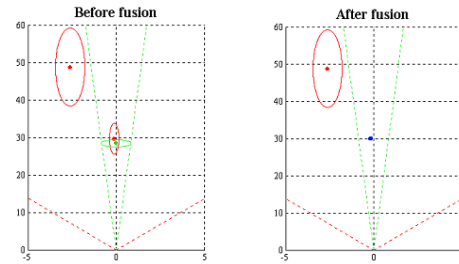


Fig. 11: Data Fusion on simple situation (red = Infrared, green = Radar, blue = dual-mode)

The vehicle positions propose different cases:

- the vehicle on the left is in the IR exclusive area: its IR track cannot be confirmed by any radar track and is passed directly through fusion,

- the vehicle on our lane is in the dual mode area: its IR and Radar tracks are close enough and associated to build a dual mode track (blue in the right hand side map).

Our observation confirms expectations: the error area of the dual mode track is far smaller than its single sensor counterparts. This is a mathematical consequence of the combination of two gaussian distributions.

Overtaking of a vehicle This case of overtaking illustrates the complementarity of Infrared and Radar. We approach the preceding vehicle (figure 12) and then pull out (figure 13, at the beginning of the manoeuvre). With the

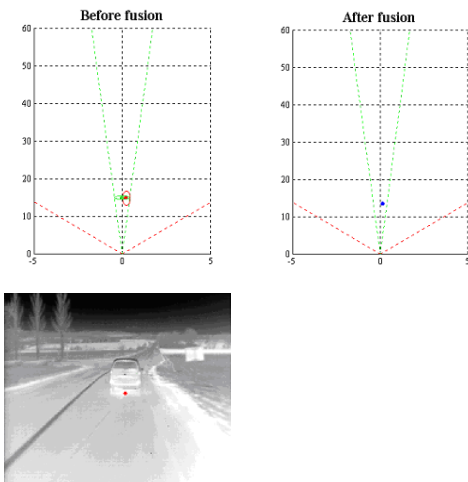


Fig. 12: Overtaking of vehicle, step 1

Radar alone, the system detects a vehicle ahead approaching until the last moment. Detection direction from Infrared influences the dual mode track, allowing to detect the drift of the vehicle, therefore no longer classified as a threat. (Although the vehicle seems to be detected out of the Radar

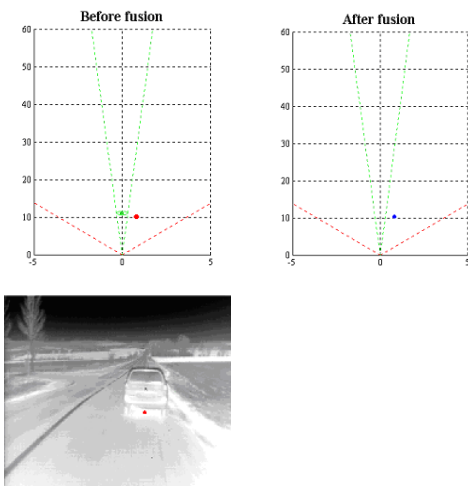


Fig. 13: Overtaking of vehicle, step 2

field in figure 13, is due to the representation: the radar exclusive area is for $-3dB$ gain, and the radar actually detects the left side of the vehicle which is overlapping the dual mode area).

Security barriers on highway The vehicle is detected by Infrared, and, being out of the dual mode area, does not require any Radar confirmation. The Radar detects the rail in the dual mode area, but IR does not confirm it, so it is discarded, therefore avoiding a false obstacle. Symmetric situations (IR and no Radar) also happen.

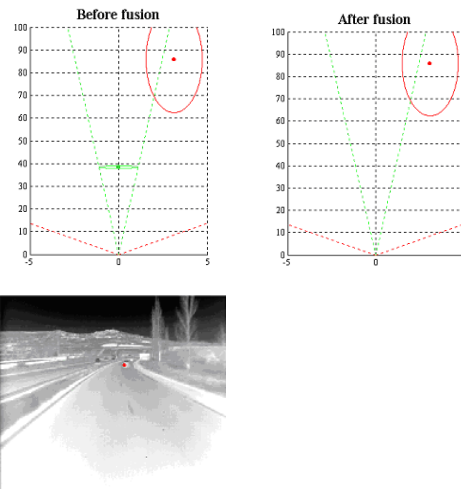


Fig. 14: Radar detection not confirmed by infrared

3.2 Fusing Radar and LIDAR tracking

Here we use the same track to track fusion method by using Radar and Lidar tracks.

3.2.1 Lidar specifications and tracking results

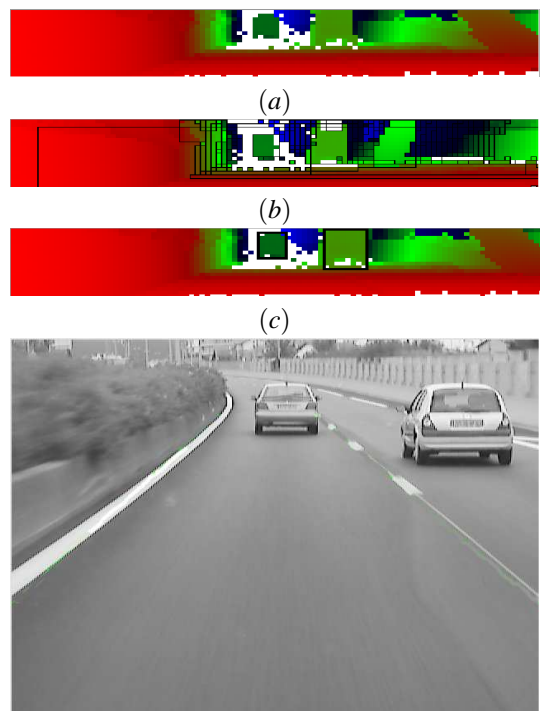


Fig. 15: 3D images segmentation and obstacle detection

The 3D-Laser Mirror Scanner LMS-Z210-60 is a surface imaging system based upon accurate distance measurement

by means of electro-optical range measurement and a two axis beam scanning mechanism.

The rangefinder system is based upon the principle of time-of-flight measurement of short laser pulses in the infrared wavelength region. Many methods for time-of-flight's calculation are described in [10]. The task of the scanner mechanism is to direct the laser beam for range measurement in a accurately defined position. The 3D images are configurable. In our approach 20lines x 103 pixels images at nearly 2Hz are used (see figure 15). The line scan mechanism (rotating polygonal four facets mirrors) provides a scan angle range about 60° fixed at a speed of 5 lines/s up to maximum 90 lines/s with an angle step width included between 0.072° and 0.36° and a readout accuracy of 0.036°. The frame scanner mechanism which is slower (1°/s up to max 20°/s) than the line scan relies on rotating the optical head together with the fast line scan. This is



Fig. 16: Implementation of LIDAR

accomplished by mounting both the line scanner mechanism and the optical head on a rotating table (0° up to max. 333°). The angle step width is 0.072° to 0.36° with an angle readout accuracy of 0.018°. This sensor is installed in the front bumper of our experimental vehicle VELAC (see figure 16). For the obstacle detection, a two parts detection algorithm is used: first the segmentation of the 3D image in regions and second the recognition of the obstacle (particularly road vehicles) among these regions. A region growing algorithm is used to perform the segmentation of the 3D image (see figure 15(b)). A region, including shots located at nearly the same distance z with a tolerance tz , is parameterized by a vector $O_i = (\text{width}, \text{height}, x_{obs}, y_{obs}, z_{obs})$ where $x_{obs}, y_{obs}, z_{obs}$ is the position of target's center in the laser scanner reference. These characteristics are then compared to a car model. If parameters of a region are close to those of the model, this region is declared as an obstacle (see figure 15(c)). After detection of different obstacles, we are able to track them in consecutives frames using a constant velocity Kalman filter.

3.2.2 Radar specifications and tracking results

see §3.1.1

3.2.3 Data fusion and results

Radar and Lidar complement each other. Indeed, Lidar have a larger field of view than the Radar (see figure 17). Its side and longitudinal resolution is better and furthermore the recognition obstacle degree is higher for Lidar. In the other side, data sample for Radar is 8ms while it is 500ms for Lidar. Moreover, Radar is insensitive to atmospheric

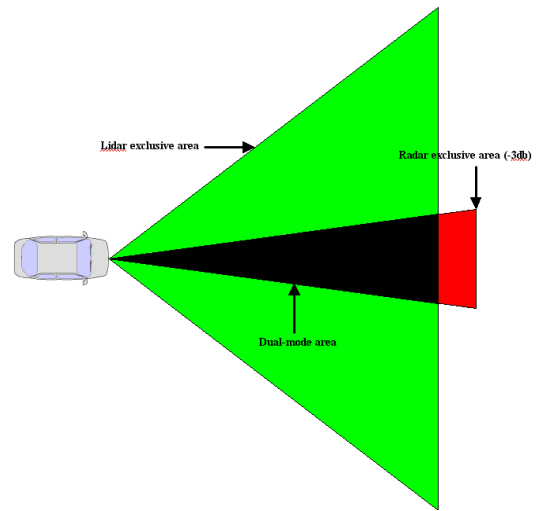


Fig. 17: Areas covered by Lidar/Radar system

conditions as shown in figure 7 in foggy condition.

For results: Lidar and Radar tracks are respectively represented in green and red. Furthermore, with calibration between Lidar and visible camera we can project obstacles in visible camera image (green circle). When tracks are associated, it is shown with a little blue rectangle.

Simple situation On figure 18, we observe two vehicles in the image. After sensor processing step, Lidar and Radar send to the fusion module the produced tracks.

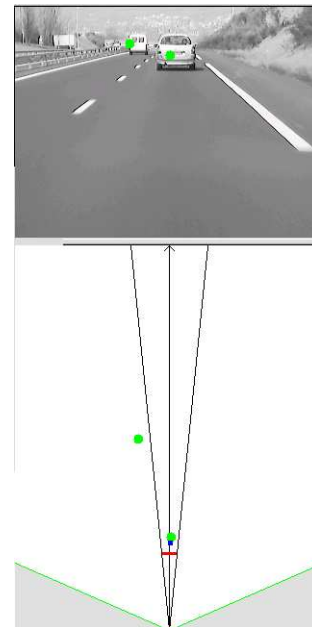


Fig. 18: Track fusion on simple situation

The vehicle positions propose different cases:

- the vehicle on the left is in the Lidar exclusive area; its Lidar track cannot be confirmed by any radar track and is passed directly through fusion,
- the vehicle on our lane is in the dual mode area: its

Lidar and Radar tracks are associated to build a dual mode track.

Two fused tracks We show that we are able to fuse many tracks. These results present the geometrical complementarity of the two sensors. Indeed, with only Radar we are not able to say if the obstacle is on the right or left side of our testbed vehicle. We can see on figure 19 that Lidar permits to improve the side resolution of the fused tracks. Like for result present figure 13, vehicles seem to be detected out of the Radar exclusive area. It is also due to representation.

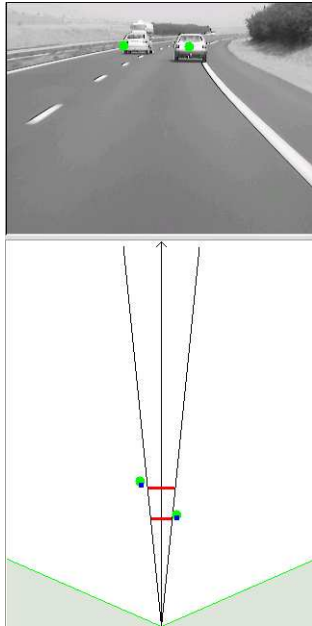


Fig. 19: Two fused tracks

4 Conclusions

We have presented a data fusion method and its application to the obstacle detection problem in road situation. A data fusion module developed and integrated in two systems that work in real-time aboard our testbed vehicle. PAROTO system combines infrared imagery (accurate direction measurement, day / night and adverse weather conditions insensitivity) with Radar (accurate radial distance and speed), to perform obstacle avoidance. Results show the quality of their collaboration through the fusion module, improving interpretation of the situation and reducing false alarm rate. We have also presented a system combining Radar and Lidar tracking which improves the environment interpretation. The benefit of fusion has been proven, and is now being further evaluated through intensive experiments.

Acknowledgements

This study has been partially supported by the French Ministry of Research, within the framework of the PAROTO project.

References

- [1] J. Laneurit, C. Blanc, R. Chapuis, and L. Trassoudaine. Multisensorial data fusion for global vehicle and obstacles absolute positioning. In *IV 2003(IEEE Int. Conf. on Intelligent Vehicles)*, Columbus (USA), June 2003.
- [2] C. Stiller, J. Hipp, C. Rssig, and A. Ewald. Multisensor obstacle detection and tracking. *Image and Vision Computing*, Volume(18):389–396, 2000.
- [3] B. Steux, C. Laugeau, L. Salesse, and D. Wautier. Fade : A vehicle detection and tracking system featuring monocular color vision and radar data fusion. In *IV 2002 (IEEE Int. Conf. on Intelligent Vehicles)*, Versailles (France), June 2002.
- [4] B F. La Scala and A. Farina. Choosing track association method. *Information Fusion*, Volume(3):119–133, 2002.
- [5] J.B. Gao and C.J. Harris. Some remarks on kalman filters for the multisensor fusion. *Information Fusion*, Volume(3):191–201, 2002.
- [6] Y. Bar-Shalom and T.E. Fortmann. *Tracking and data association*, volume 179. Mathematics in science and engineering, 1988.
- [7] Y. Le Guilloux, J. Lonnoy, R. Moreira, MP. Bruyas, A. Chapon, and H. Tattegrain. Paroto project : the benefit of infrared imagery for obstacle avoidance. In *IV 2002 (IEEE Int. Conf. on Intelligent Vehicles)*, Versailles (France), June 2002.
- [8] Y. Le Guilloux, J. Lonnoy, and R. Moreira. Infrared image processing for obstacle avoidance. In *AMAA 2003 (Advanced Microsystems for Automotive Applications)*, Berlin (Germany), May 2003.
- [9] Y. Le Guilloux, J. Lonnoy, R. Moreira, C. Blanc, J. Gallice, L. Trassoudaine, H. Tattegrain, MP. Bruyas, and A. Chapon. Paroto project : infrared and radar data fusion for obstacle avoidance. In *AMAA 2004 (Advanced Microsystems for Automotive Applications)*, Berlin (Germany), March 2004.
- [10] J. Hancock. *Laser intensity-based obstacle detection and tracking*. PhD thesis, The robotics institute, Carnegie Mellon university, Pittsburgh, USA, 1999.